

UC Riverside

UC Riverside Previously Published Works

Title

Flame Synthesis of Nanomaterials

Permalink

<https://escholarship.org/uc/item/4qq703wb>

ISBN

9789813277830

Author

JUNG, HEEJUNG

Publication Date

2019-10-01

DOI

10.1142/9789813277847_0008

Peer reviewed

CHAPTER 8

Flame Synthesis of Nanomaterials

HEEJUNG JUNG

Department of Mechanical Engineering, University of California,
Riverside, CA, 92521, USA

8.1. Introduction

Nanoparticles can be synthesized via multiple methods in gas phase. Various gas-phase synthesis processes have distinctive reaction environments, phase of precursors, and reaction routes but they all have a common procedure of applying energy into the precursor/reactants and let the energy leave by heat transfer in the post-reaction zone as shown in Fig. 8.1.

Several gas-phase synthesis processes have been developed to provide different reaction environments for the formation of nanoparticles. Some of those processes are listed below and will be discussed in more detail in the following sections:

- Spray pyrolysis (liquid-phase precursor);
- Flame spray pyrolysis (FSP, liquid-phase precursor);
- Flame synthesis using premixed flame burner (liquid- or gas-phase precursor);

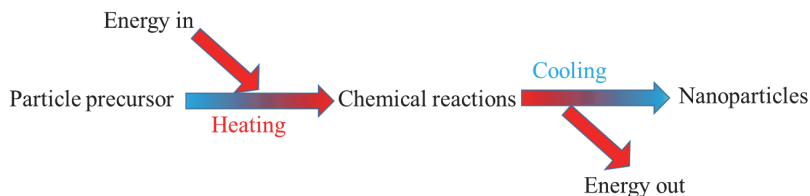


Fig. 8.1. Schematic diagram of the gas-phase nanoparticle synthesis process.

- Flame synthesis using diffusion flame burner (liquid- or gas-phase precursor);
- Spark discharge (solid-phase precursor).

8.2. Spray Pyrolysis

Precursors of particles are dissolved in the choice of solvent so that precursors are in liquid form. Water and alcohols are typically used as solvents. Concentrations of the precursor and choice of the solvent makes difference in the resulting particles synthesized. Liquid precursors along with the solvent are sprayed via multiple methods (Fig. 8.2). Mechanical spraying such as sonication tends to generate droplets in 10–30 μm size range while a special spraying technique, such as electro-spraying, generates droplets as small as few nanometers. These droplets are fed into a tube flow reactor for which temperature and residence time profiles are well characterized. Oftentimes, radial temperature gradients are ignored and tubes with relatively high aspect ratio are preferred for that reason. Competition between evaporation of solvent and diffusion of solute results in diverse particles in shape, size, and morphology as illustrated in Fig. 8.3 by Okuyama and Lenggoro.¹ For the pyrolysis reaction, N_2 and H_2 are often used as carrier gas and for the production of oxides, air is used as carrier gas.

Kim *et al.*² demonstrated the morphology of aluminum oxide can be controlled by using leachable inorganic matrix which can be washed out in the post-processing. Figure 8.4 shows a diverse possible morphology of aluminum oxide as a function of synthesis conditions.

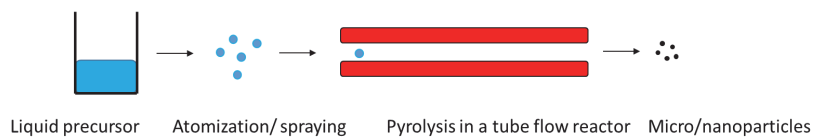


Fig. 8.2. Schematic diagram of spray pyrolysis.

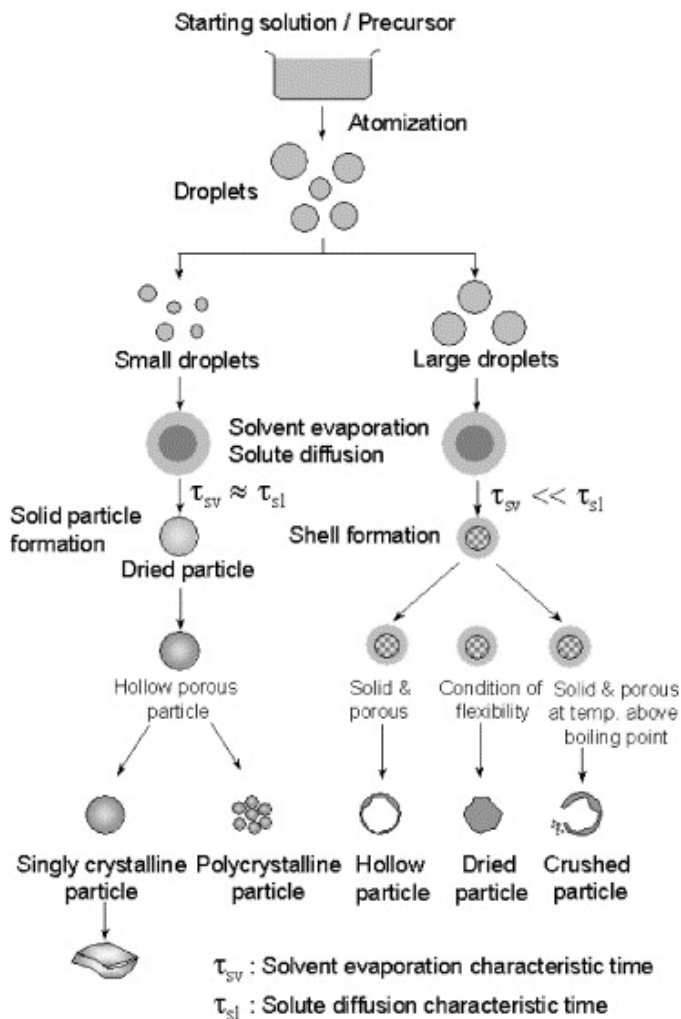


Fig. 8.3. Morphological variation of particles by spray pyrolysis.¹

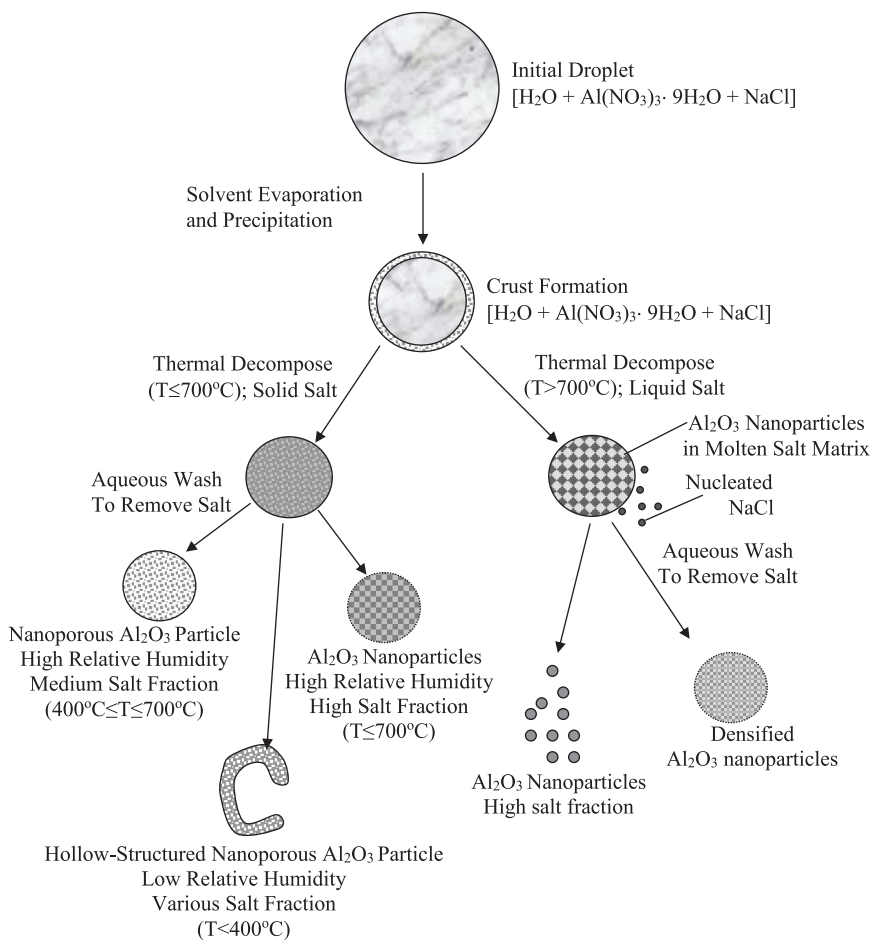


Fig. 8.4. Possible routes to synthesize nanoporous aluminum oxide particle.⁸

8.3. Flame Spray Pyrolysis

There are a few types of FSP methods depending on the configuration of flame and spraying approach. In FSP, liquid precursors are nebulized and fed into the flame. Nebulized droplets quickly vaporize under hot environment and particles are formed as temperature decreases due to cooling and dilution.

8.3.1. FSP with turbulent flame assisted by CH_4/O_2 flamelets

Pratsinis at ETH has pioneered and contributed significantly to the development of FSP. Figure 8.5 shows the design of his FSP apparatus. Particle precursors dissolved in flammable solvents such as hexane and alcohols are fed through a capillary tube by a syringe pump. Air/ O_2 / CH_4 gasses are fed through a co-axial capillary tube and they nebulize liquid precursors into droplets at the tip of the capillary tube. CH_4/O_2 flamelets are concentrically arranged around the nozzle exit to help sustain the turbulent flame which otherwise will extinguish.

There are several parameters that control the synthesis process. Oxidant flow rates determine the size of droplets. Combination of oxidant and fuel flow rates along with corresponding oxidant and

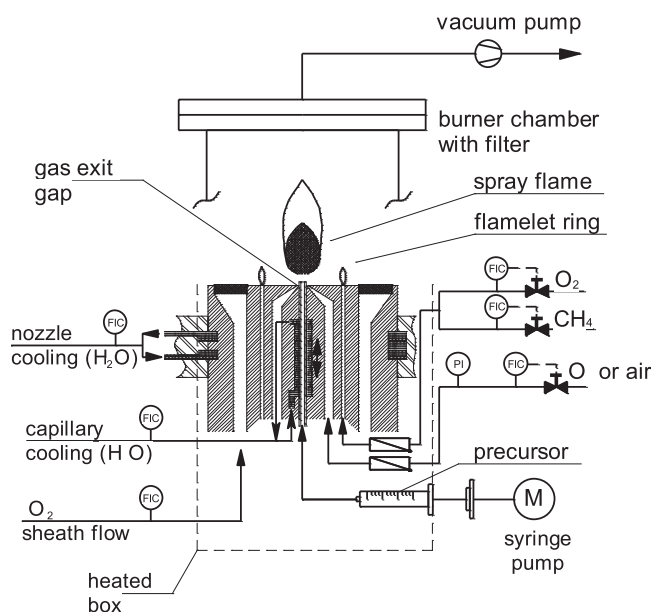


Fig. 8.5. Pratsinis' FSP experimental setup.³

fuel species determine the flame structure. Droplets quickly evaporate and contribute to the formation of a turbulent flame. Vaporized precursors form particles that undergo coagulation and coalescence depending on time and temperature history of the turbulent flame. Mädler *et al.*³ found that specific surface area increases with increasing oxidant flow rate at low oxidant flow rates as the spray flame length is reduced leading to shorter residence time allowing less time for particle growth.

One of the advantages of the FSP method is that the process can be scaled up for a large-scale production of nanomaterials. Pratisnis is one of very few scientists who successfully demonstrated the scale-up process of the FSP method.⁴ Stark *et al.*⁴ and Mueller *et al.*⁵ showed that the production rate can be increased by two orders of magnitude when such approaches are taken.

8.3.2. FSP with oxyhydrogen turbulent flame

Dosev *et al.*⁶ developed a different type of FSP setup as shown in Fig. 8.6. First, they nebulized the liquid precursor using the oxidant

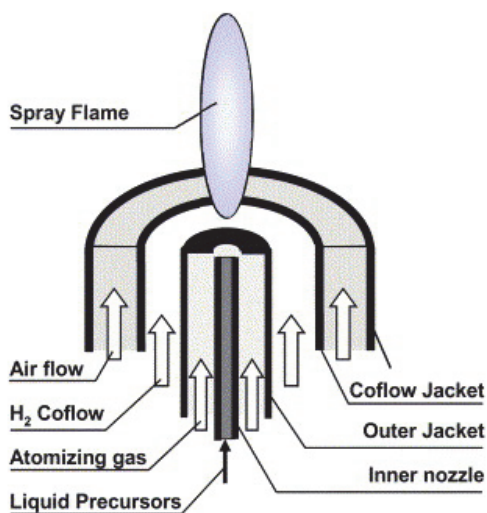


Fig. 8.6. Dosev *et al.*'s⁶ FSP experimental setup.

flow the same way as Pratisnis' setup. Next, they placed another co-axial flow with hydrogen to establish oxy-hydrogen flame where liquid precursors vaporize and undergo reaction. Oxy-hydrogen flame provides carbonless environment for nanoparticle synthesis, which is a big difference from the Pratsinis' setup which uses hydrocarbon flame. They added another co-flow of air at the outer rim of the burner to stabilize the flame.

They dissolved europium nitrate and yttrium nitrate in the ethanol solution, and used a syringe pump to feed at 40 mL/h. Air at 2 lpm was used to nebulize the precursor solution and hydrogen flow of 2 lpm along with 10 lpm co-flow air established hydrogen flame for synthesis. The temperature of the oxy-hydrogen flame was measured as 2100°C. A cold finger was used to collect resulting europium-doped yttria particles by thermophoresis.

8.3.3. FSP with oxyhydrogen turbulent flame:

Use of a spray gun

Tikkanen *et al.*⁷ developed a spray flame gun to synthesize nanoparticles as shown in Fig. 8.7. Liquid precursor is fed through a capillary tube and co-flowing hydrogen gas sprays (or nebulizes) liquid precursor into droplets. Additional co-flowing oxygen provides oxidants so that a turbulent spray flame can be sustained for a thermochemical nanoparticle synthesis process. They found atomized droplet size

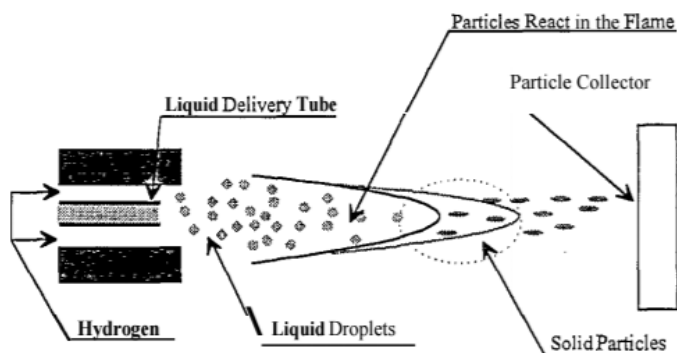


Fig. 8.7. Schematics of spray flame gun.⁷

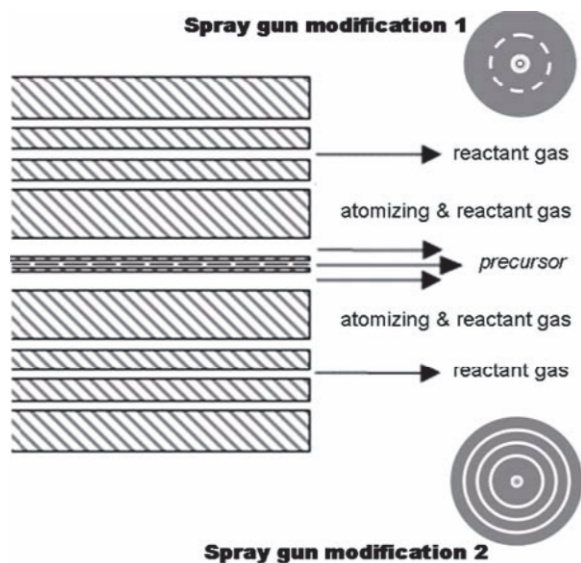


Fig. 8.8. Modified spray gun design by Keskinen.⁸

distribution can be varied by changing atomizer parameters such as atomizing gas flow rate, liquid type and liquid feed rate. Flame length is controlled by gas flow rates and a solvent is used to dissolve precursor materials. An organic solvent such as isopropanol extends the flame length.

Keskinen⁸ modified the spray gun design as shown in Fig. 8.8 to further control turbulent flame, droplet size, and synthesis process. Additional co-flow with nitrogen enables to control the flame temperature profile. She mentioned some large residual particles especially at high production rate poses a problem that must be solved. She synthesized various nanoparticles including metals, metal oxides, silver/palladium, and silica using the setup.

8.3.4. *FSP with turbulent flame: Use of three co-axial flows*

Zheng *et al.*⁹ developed a co-axial type FSP setup as shown in Fig. 8.9. It has more complicated geometry than previous FSPs by

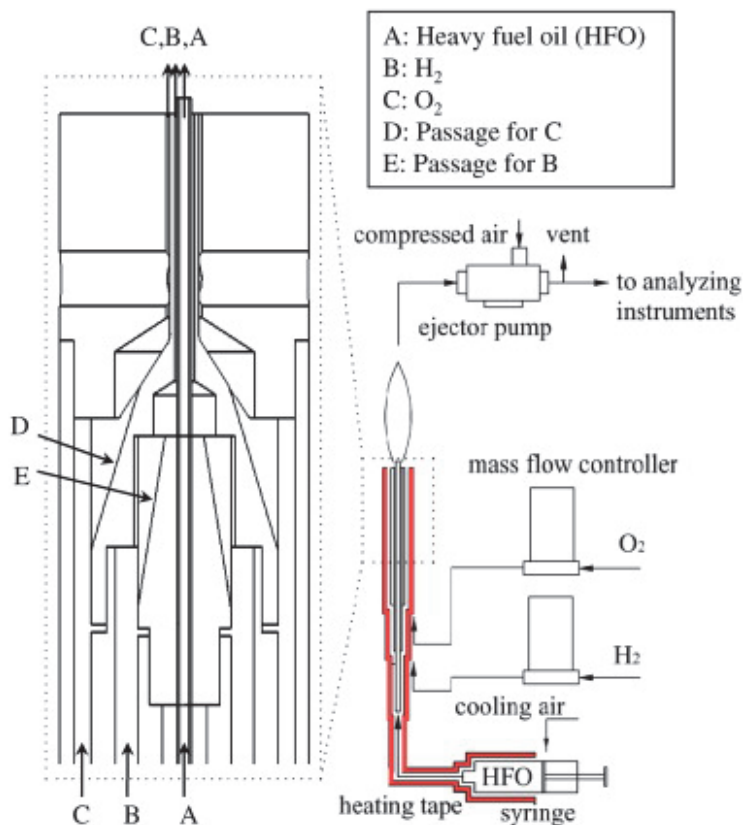


Fig. 8.9. Schematic diagram of Zheng *et al.*'s⁹ FSP setup. The red part shows that the FSP setup is heated by a heating tape.

others. Set-screws were used to center the capillary tube in the middle and internal channels were used to reduce tubes into capillary tubes. Most of parts were made with commercially available stainless steel tubing but special machining was required to enable channel flows. This is a research purpose FSP which comes with experimental flexibility. Velocity or flow rate of co-flows of fuel gas and oxidants are variable to find optimum synthesis conditions. Since all materials are made of stainless steel and the FSP setup is relatively small, the whole FSP setup can be heated up when precursors are less volatile, which was the case for Ref. 9 using heavy fuel oil as a precursor.

Downside of this burner is that the configuration of capillary tubes is crowded in a very small area and therefore the innermost tube, where liquid precursor comes out, can often be clogged by thermophoresis during the synthesis process.

8.4. Flame Synthesis Using Premixed Flame Burner

Premixed flame provides well-defined temperature and flow conditions along with uniform flame environment compared to other flame synthesis methods. While spray and diffusion flames are at least two dimensional, the premixed flame can be assumed as one dimension, i.e., temperature and flow conditions change as a function of flame height only. Another advantage is that one can model the flame conditions accurately for premixed flames meaning the flame synthesis process can also be modeled under right boundary conditions. Nikraz *et al.*¹⁰ and Tolmachoff *et al.*¹¹ stabilized a premixed flame, as shown in Fig. 8.10, using $C_2H_2/Ar/O_2$ near the surface of the metal plate where the synthesized particles need to be deposited. Titanium tetraisopropoxide (TTIP), a precursor for titania, was injected into the carrier gas and fed into the flame. To prevent condensation of TTIP, the fuel lines were heated. Argon was used as a diluent to

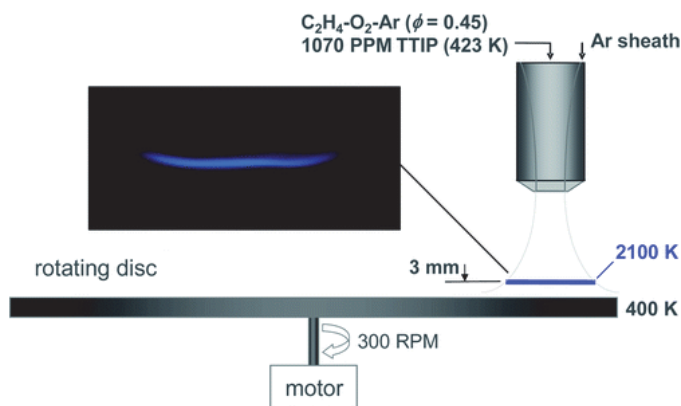


Fig. 8.10. Premixed flame setup to synthesize and deposit titania nanoparticles.¹¹

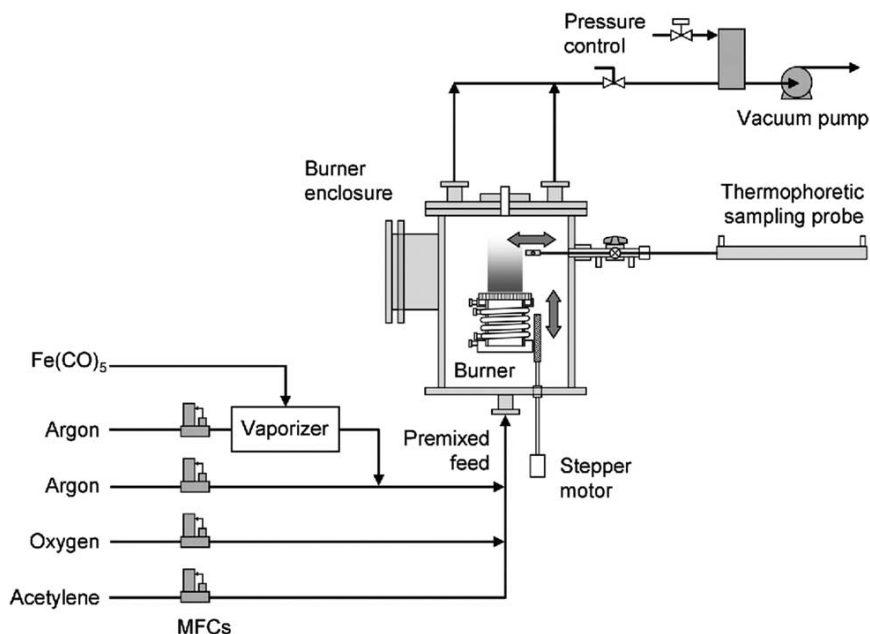


Fig. 8.11. Configuration of low pressure premixed flame burner for CNT synthesis.¹²

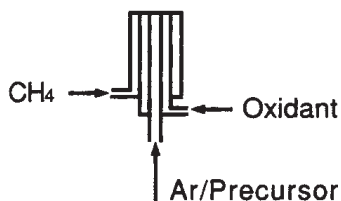
control flame temperatures and synthesized particles were deposited to the substrate by thermophoresis.

Height *et al.*¹² used a premixed acetylene/oxygen/argon flame to synthesize carbon nanotubes as shown in Fig. 8.11. Iron pentacarbonyl was carried by argon to provide seeding materials into the flame. They found unique synthesis conditions, where the CNT formation is promoted instead of the soot formation at an equivalence ratio between 1.6 and 1.8.

8.5. Flame Synthesis Using Diffusion Flame Burner

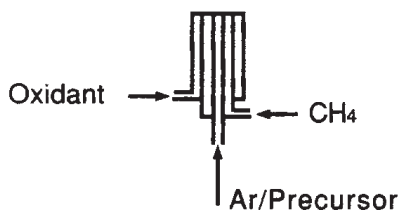
It is relatively easier to build a diffusion flame burner and so the history of flame synthesis using a diffusion flame is long. Typically, precursor vapors are carried by diluent gas which controls flame temperatures. Zhu and Pratsinis¹³ synthesized silica and tin oxide using methane diffusion flame and inverted diffusion flame as shown in

Flame IDF



(a)

Flame DF



(b)

Fig. 8.12. Diffusion flame configuration of Ref. 13 for particle synthesis.

Fig. 8.12. Pratsinis¹⁴ published a review paper with focus on ceramic particles. Later on, Wegner and Pratsinis¹⁵ provided key parameters (burner out velocity difference of oxygen and fuel flow) to control a scale-up of the synthesis process.

Lee and Choi¹⁶ applied laser beam into the flame to control the crystalline phase of nanocrystalline nanoparticles as shown in Fig. 8.13. Heating and subsequent cooling could control the degree of coalescence of particles and resulted in smaller and unagglomerated particles.

8.6. Particle Synthesis Using Spark Discharge

Spark discharge occurs when two facing electrodes form a conducting channel due to gas breakdown at high electric bias voltage. This phenomenon is fast, local, and provides extremely high temperatures near the discharge. The high temperature and subsequent adiabatic

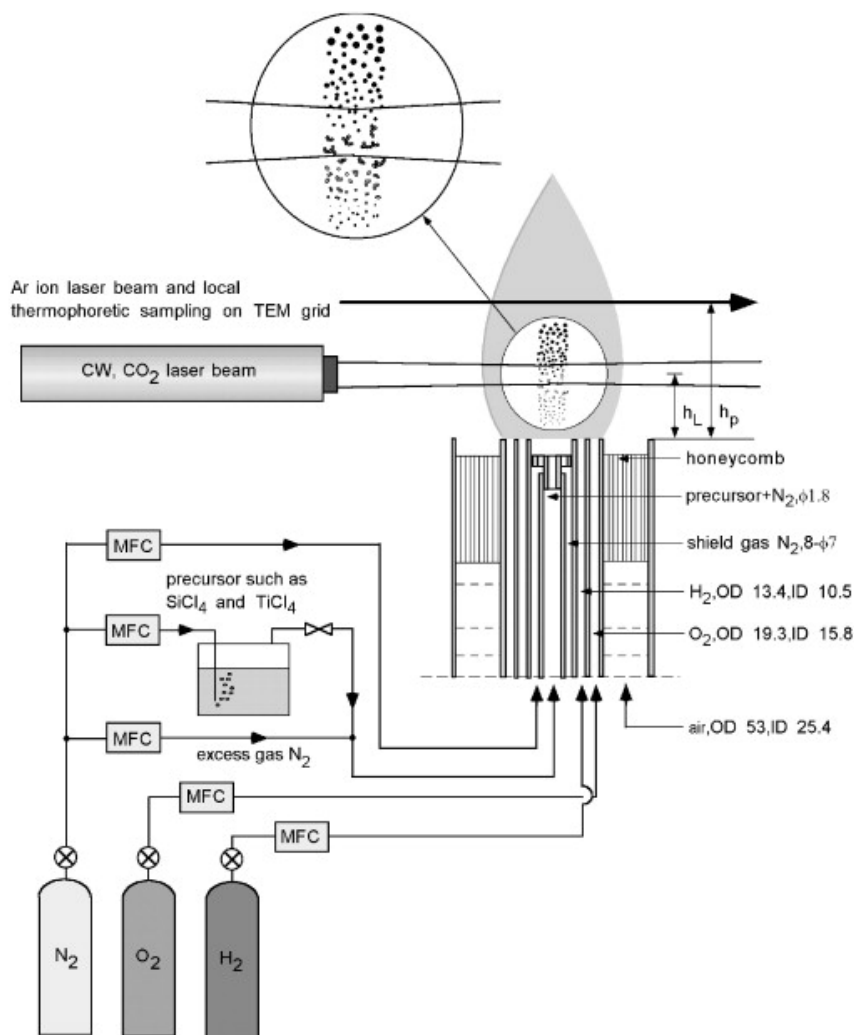


Fig. 8.13. Coalescence-enhanced particle synthesis using diffusion flame.¹⁶

cooling provide a unique condition for electrode materials to evaporate and form nanoparticles. Tabriz *et al.*¹⁷ conducted a systematic study to understand the influence of key parameters on primary particle size and mass production rate. His setup is shown in Fig. 8.14. When carrier gas flows, the resulting particle size distribution is

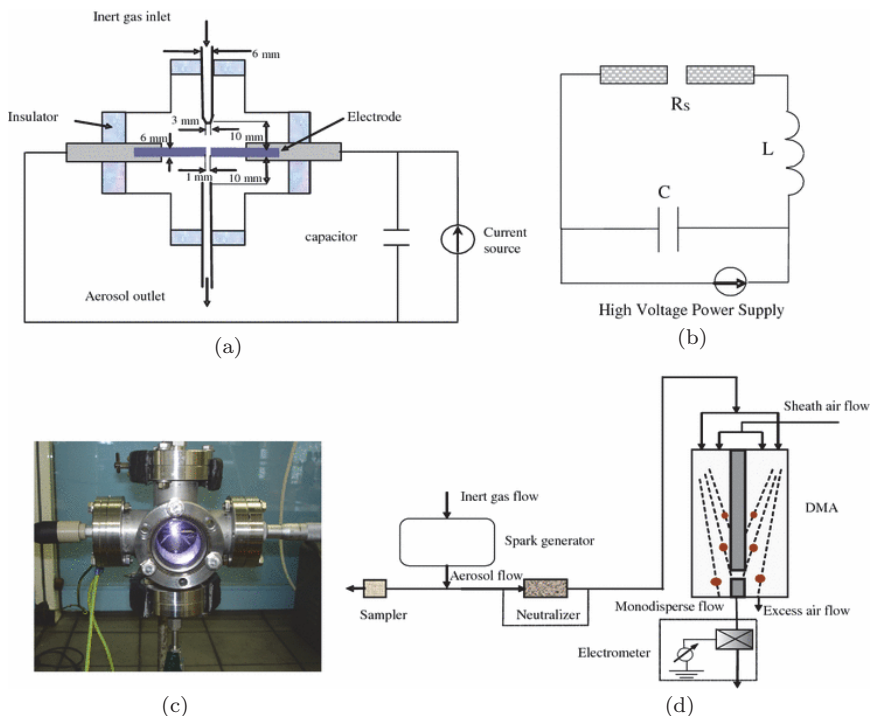


Fig. 8.14. Spark discharge setup for nanoparticle synthesis.¹⁷

narrow and the mode diameter is in few nanometers. When there is no gas flow, an aerogel of web-like structure forms opening possibilities of producing arbitrary mixtures of materials on a nanoscale.

References

1. Okuyama, K. and Lenggoro, I. W. (2003). Preparation of nanoparticles via spray route, *Chemical Engineering Science* **58**(3), pp. 537–547.
2. Kim, S., Liu, B. and Zachariah, M. (2002). Synthesis of nanoporous metal oxide particles by a new inorganic matrix spray pyrolysis method, *Chemistry of Materials* **14**(7), pp. 2889–2899.
3. Mädler, L., Kammler, H., Mueller, R. and Pratsinis, S. (2002). Controlled synthesis of nanostructured particles by flame spray pyrolysis, *Journal of Aerosol Science* **33**(2), pp. 369–389.
4. Stark, W. J., Kammler, H. K., Strobel, R., Günther, D., Baiker, A. and Pratsinis, S. E. (2002). Flame-made titania/silica epoxidation catalysts: Toward

- large-scale production, *Industrial & Engineering Chemistry Research* **41**(20), pp. 4921–4927.
5. Mueller, R., Mädler, L. and Pratsinis, S. E. (2003). Nanoparticle synthesis at high production rates by flame spray pyrolysis, *Chemical Engineering Science* **58**(10), pp. 1969–1976.
 6. Dosev, D., Guo, B. and Kennedy, I. M. (2006). Photoluminescence of Eu^{3+} : Y_2O_3 as an indication of crystal structure and particle size in nanoparticles synthesized by flame spray pyrolysis, *Journal of Aerosol Science* **37**(3), pp. 402–412.
 7. Tikkanen, J., Gross, K., Berndt, C., Pitkänen, V., Keskinen, J., Raghu, S., *et al.* (1997). Characteristics of the liquid flame spray process, *Surface and Coatings Technology* **90**(3), pp. 210–216.
 8. Keskinen, H. (2007). *Synthesis of nanoparticles and preparation of deposits by liquid flame spray*, Tampere University of Technology.
 9. Zheng, Z., Tang, X., Asa-Awuku, A. and Jung, H. S. (2010). Characterization of a method for aerosol generation from heavy fuel oil (HFO) as an alternative to emissions from ship diesel engines, *Journal of Aerosol Science* **41**(12), pp. 1143–1151.
 10. Nikraz, S., Phares, D. J. and Wang, H. (2012). Mesoporous titania films prepared by flame stabilized on a rotating surface: Application in dye sensitized solar cells, *The Journal of Physical Chemistry C* **116**(9), pp. 5342–5351.
 11. Tolmachoff, E., Memarzadeh, S. and Wang, H. (2011). Nanoporous titania gas sensing films prepared in a premixed stagnation flame, *The Journal of Physical Chemistry C* **115**(44), pp. 21620–21628.
 12. Height, M. J., Howard, J. B., Tester, J. W. and Vander Sande, J. B. (2004). Flame synthesis of single-walled carbon nanotubes, *Carbon* **42**(11), pp. 2295–2307.
 13. Zhu, W. and Pratsinis, S. E. (1997). Synthesis of (SiO_2) and (SnO_2) particles in diffusion flame reactors, *American Institute of Chemical Engineers. AIChE Journal* **43**(11A), p. 2657.
 14. Pratsinis, S. E. (1998). Flame aerosol synthesis of ceramic powders, *Progress in Energy and Combustion Science* **24**(3), pp. 197–219.
 15. Wegner, K. and Pratsinis, S. E. (2003). Scale-up of nanoparticle synthesis in diffusion flame reactors, *Chemical Engineering Science* **58**(20), pp. 4581–4589.
 16. Lee, D. and Choi, M. (2002). Coalescence enhanced synthesis of nanoparticles to control size, morphology and crystalline phase at high concentrations, *Journal of Aerosol Science* **33**(1), pp. 1–16.
 17. Tabrizi, N. S., Ullmann, M., Vons, V., Lafont, U. and Schmidt-Ott, A. (2009). Generation of nanoparticles by spark discharge, *Journal of Nanoparticle Research*, **11**(2), p. 315.